Synthesis, structure, and magnetic properties of LaTMg and CeTMg (T = Pd, Pt, Au)

2002 J. Phys.: Condens. Matter 14 5173

(http://iopscience.iop.org/0953-8984/14/20/312)

INSTITUTE OF PHYSICS PUBLISHING JOURNAL OF PHYSICS: CONDENSED MATTER

J. Phys.: Condens. Matter **14** (2002) 5173–5186 PII: S0953-8984(02)34553-3

Synthesis, structure, and magnetic properties of LaTMg and CeTMg (T = Pd, Pt, Au)

B J Gibson[1], A Das[1,3], R K Kremer[1], R-D Hoffmann[2] and R Pöttgen[2]

[1] Max-Planck-Institut für Festkörperforschung, Heisenbergstraße 1, D-70569 Stuttgart, Germany
[2] Institut für Anorganische und Analytische Chemie, Universität Münster, Wilhelm-Klemm Straße 8, D-48149 Münster, Germany

Received 5 March 2002
Published 9 May 2002
Online at stacks.iop.org/JPhysCM/14/5173

Abstract

The title compounds were prepared from the elements by reactions in sealed tantalum tubes in a water-cooled sample chamber of a high-frequency furnace. They crystallize with the ZrNiAl-type structure, space group $P\bar{6}2m$. The structures of the cerium compounds were refined from single-crystal x-ray diffraction data: $a = 767.3(1)$ pm, $c = 410.37(4)$ pm, $wR2 = 0.0324$, 521 F^2-values for CePdMg; $a = 755.02(7)$ pm, $c = 413.82(4)$ pm, $wR2 = 0.0393$, 514 F^2-values for CePtMg; and $a = 774.1(3)$ pm, $c = 421.6(1)$ pm, $wR2 = 0.0355$, 395 F^2-values for CeAuMg, with 14 variables for each refinement. The palladium compound shows a small homogeneity range: $CePd_{1+x}Mg_{1-x}$. The structures contain two crystallographically different transition metal sites T1 and T2 which are located in tri-capped trigonal prisms: $[T1Mg_6Ce_3]$ and $[T2Ce_6Mg_3]$. Magnetic susceptibility and heat capacity measurements reveal long-range magnetic ordering at 2.1(2) K for CePdMg, 3.6(2) K for CePtMg, and 2.0(2) K for CeAuMg. Curie–Weiss behaviour at higher temperatures shows that the cerium ions are in the 3+ oxidation state. The isotypic LaTMg compounds are Pauli paramagnetic down to lowest temperatures ($T = 0.3$ K). All the compounds, RETMg (RE = La, Ce; T = Pd, Pt, Au) show metallic behaviour.

1. Introduction

The families of intermetallic CeTX and Ce_2T_2X (T = transition metal; X = element of the III, IV, or V main group) compounds have been intensively investigated in recent years as regards their greatly varying magnetic and electrical properties [1–8]. Corresponding systems with a divalent main group element (magnesium or cadmium), however, have scarcely been studied.

Some detailed investigations were performed for the Heusler phases, $REAg_xMg_{3-x}$ (RE = rare-earth element) [9] with the focus on the ordering of silver and magnesium atoms. Later, equiatomic RETMg, RETCd, and RETHg were reported by Iandelli [10], but systematic studies as regards phase diagrams have only been performed for the Ce–Cu–Cd system [11].

[3] On leave from Bhabha Atomic Research Centre, Bombay, India.

We have recently started a more systematic investigation of these magnesium and cadmium compounds [7, 8] and discovered intermediate-valence $Ce_2Ni_{1.88}Cd$ [7], as well as Ce_2T_2Mg (T = Ni, Cu, Pd), and Ce_2T_2Cd (T = Pd, Pt, Au) with ordered U_3Si_2-type structure. Detailed physical property investigations for the equiatomic compounds LaAgMg, CeAgMg, EuAgMg, YbAgMg, and EuAuMg have been reported recently [12]. Herein, we report on the synthesis, structure refinements, and physical properties of the equiatomic magnesium compounds LaTMg and CeTMg (T = Pd, Pt, Au). So far, only x-ray powder data [10] for LaPdMg and CePdMg, and preliminary magnetic data for CePdMg [13] have been published.

2. Experimental details

The starting materials for the preparation of LaTMg and CeTMg (T = Pd, Pt, Au) were ingots of lanthanum and cerium (Johnson-Matthey, >99.9%), palladium and platinum powder (Degussa, 200 mesh, >99.9%), gold wire (Degussa, diameter 1 mm, >99.9%), and a magnesium rod (Johnson-Matthey, diameter 16 mm, >99.95%). The lanthanum and cerium ingots were cut into small pieces under paraffin oil. These pieces were washed with *n*-hexane and kept in Schlenk tubes under vacuum. The paraffin oil and *n*-hexane were dried over sodium wire. Small lanthanum and cerium pieces were arc-melted under argon (600 mbar) in a first step in order to obtain compact buttons. The argon was purified over titanium sponge (900 K), silica gel, and molecular sieves. Details of the melting apparatus are given in [14]. In a second step the lanthanum or cerium buttons (about 500 mg) were mixed with the respective transition metal and magnesium pieces in the ideal 1:1:1 atomic ratios and sealed in small tantalum tubes (tube volume about 1 cm^3) under an argon atmosphere of about 800 mbar.

The tantalum tubes were placed in a water-cooled quartz glass sample chamber in a high-frequency furnace (KONTRON Roto-Melt, 1.2 kW) under flowing argon [15]. They were first heated for about 1 min with the maximum power output of the generator (about 1500 K) and subsequently annealed at about 900 K for another 2 h. The reaction between the three elements was visible as a short glowing of the tubes. After the annealing procedures the samples could be easily separated from the tantalum tubes. No reactions of the samples with the tubes could be detected. Most samples were obtained in amounts of 1 g after the annealing procedures. Compact pieces of the samples are light grey with metallic lustre while the powders are dark grey. The compounds are stable in moist air. No decomposition was observed after several weeks.

Guinier powder patterns of the samples were recorded with Cu Kα_1 radiation using α-quartz (a = 491.30 pm, c = 540.46 pm) as an internal standard. The indexing of the diffraction lines was facilitated by intensity calculations [16] using the positional parameters of the refined structures. The lattice parameters (table 1) were obtained by least-squares fits of the Guinier powder data. The refined lattice parameters of LaPdMg and CePdMg are in good agreement with the data previously reported by Iandelli [10], while those reported by Geibel *et al* [13] are somewhat smaller.

Single-crystal intensity data were collected at room temperature using a four-circle diffractometer (CAD4) with graphite-monochromated Mo Kα radiation (λ = 0.710 73 pm) and a scintillation counter with pulse height discrimination. The scans were performed in the $\omega/2\theta$ mode. Empirical absorption corrections were applied on the basis of ψ-scan data.

The dc magnetic susceptibilities of polycrystalline pieces (≈150 mg) were measured using a SQUID magnetometer (MPMS, Quantum Design, Inc.) between 2 and 300 K with external magnetic flux densities between 0.001 and 7 T. Due to the low magnetic ordering temperatures of these compounds we additionally measured ac magnetic susceptibilities between 0.3 and 5 K using a home-built, top-loading, single-shot ^{3}He cryostat. Measurements were made on

Table 1. Lattice parameters of several lanthanum and cerium compounds with the hexagonal ZrNiAl-type structure.

Compound	a (pm)	c (pm)	c/a	V (nm^3)	Reference
LaPdMg	771.8(1)	414.1(1)	0.537	0.2136	[10]
LaPdMg	773.6(1)[a]	413.79(4)	0.535	0.2145	This work
CePdMg	765.1(1)	410.3(1)	0.536	0.2080	[10]
CePdMg	760	408	0.537	0.2041	[13]
CePdMg	767.3(1)	410.37(4)	0.535	0.2092	This work
LaPtMg	762.0(1)	417.48(5)	0.548	0.2099	This work
CePtMg	755.02(7)	413.82(4)	0.548	0.2043	This work
LaAuMg	781.0(1)	425.49(9)	0.545	0.2248	This work
CeAuMg	774.1(3)	421.6(1)	0.545	0.2188	This work

[a] Standard deviations in the positions of the last significant digits are given in parentheses.

polycrystalline pieces of about 500 mg using a driving frequency of 37 Hz, which generated ac fields of ≈0.3 mT. The temperature of the ^{3}He bath was determined with a calibrated Ge resistor (LakeShore) which was in close contact with the sample.

Heat capacity measurements were performed using a physical properties measurement system (PPMS, Quantum Design, Inc.) between 1.9 and 100 K. Small (≈20 mg) polycrystalline pieces of the compounds were mounted on the sample holder using minute amounts of vacuum grease (Apiezon N). The addenda heat capacity was in all cases previously measured and subtracted. We utilized the *two-tau model* [17] for all of the heat capacity measurements.

Resistivity measurements were carried out on small circular pressed pellets ($\phi = 5$ mm) using the conventional four-probe van der Pauw technique [18]. Cooling and heating curves measured between 5 and 300 K were identical within error limits.

3. Results and discussion

3.1. Structure refinements

Irregularly shaped single crystals of CePdMg, CePtMg, and CeAuMg were isolated from the crushed samples after the annealing procedures and then examined by Buerger precession photographs to establish both symmetry and suitability for intensity data collection. The photographs showed hexagonal symmetry and no systematic extinctions, compatible with space groups $P6/mmm$, $P\bar{6}2m$, and $P\bar{6}m2$, of which the non-centrosymmetric group $P\bar{6}2m$ was found to be correct during the structure refinements. All relevant crystallographic data and experimental details of the data collections are listed in table 2.

The atomic positions of GdAuIn [19] were taken as starting parameters and the three structures were successfully refined with anisotropic displacement parameters for all atoms using SHELXL-97 [20] (full-matrix least-squares refinement on F^2). The refinements readily converged to the residuals listed in table 2. During each data collection, Friedel pairs were measured in order to determine the correct absolute structure. A Flack parameter [21, 22] of 1.01(5) indicated the inverse absolute structure for CePtMg. Subsequently, we inverted the atomic positions of CePtMg and refined the correct absolute structure (table 3).

The occupancy parameters were varied in separate series of least-squares cycles in order to check for deviations from the ideal compositions. For CePtMg and CeAuMg all sites were fully occupied within two standard deviations and in the final cycles the ideal occupancies were assumed again. The first palladium-containing single crystal was taken from an annealed sample of the starting composition Ce:Pd:Mg = 2:2:1. The 3g Mg site of this crystal showed

Table 2. Crystal data and structure refinements for CePdMg, CePtMg, and CeAuMg (space group $P\bar{6}2m$, $Z = 3$).

Empirical formula	CePdMg	CePtMg	CeAuMg
Molar mass (g mol^{-1})	270.83	359.52	361.40
Calculated density (g cm^{-3})	6.45	8.77	8.23
Crystal size (μm^3)	$10 \times 40 \times 40$	$15 \times 25 \times 30$	$20 \times 45 \times 60$
Transmission ratio (max/min)	1.64	2.86	3.03
Absorption coefficient (mm^{-1})	22.4	67.6	65.5
$F(000)$	348	444	447
θ-range for data collection	3°–40°	3°–40°	3°–35°
Range in hkl	$\pm13, \pm13, \pm7$	$\pm13, \pm13, \pm7$	$\pm12, \pm12, \pm6$
Total No of reflections	2675	5108	3864
Independent reflections	521 ($R_{\rm int} = 0.0501$)	514 ($R_{\rm int} = 0.0868$)	395 ($R_{\rm int} = 0.0612$)
Reflections with $I > 2\sigma(I)$	474 ($R_{\rm sigma} = 0.0285$)	449 ($R_{\rm sigma} = 0.0361$)	388 ($R_{\rm sigma} = 0.0211$)
Data/restraints/parameters	521/0/14	514/0/14	395/0/14
Goodness-of-fit on F^2	1.110	1.323	1.168
Final R-indices ($I > 2\sigma(I)$)	$R1 = 0.0184$	$R1 = 0.0223$	$R1 = 0.0146$
	$wR2 = 0.0299$	$wR2 = 0.0340$	$wR2 = 0.0346$
R-indices (all data)	$R1 = 0.0251$	$R1 = 0.0353$	$R1 = 0.0156$
	$wR2 = 0.0324$	$wR2 = 0.0393$	$wR2 = 0.0355$
Extinction coefficient	0.0068(5)	0.0021(3)	0.0150(6)
Absolute structure parameter	−0.03(2)	−0.02(1)	−0.02(1)
Largest diffraction peak and hole	1.08 and −1.27 e Å^{-3}	4.07 and −3.76 e Å^{-3}	1.08 and −1.56 e Å^{-3}

Table 3. Atomic coordinates and isotropic displacement parameters (pm^3) for CePdMg, CePtMg, and CeAuMg (space group $P\bar{6}2m$).

Atom	Wyckoff site	x	y	z	U_{11}	U_{22}	U_{33}	U_{12}	$U_{\rm eq}^{\rm a}$
CePdMg									
Ce	3f	0.583 62(5)	0	0	111(1)	118(2)	107(1)	59(1)	111(1)
Pd1	1a	0	0	0	164(2)	U_{11}	99(3)	82(1)	142(2)
Pd2	2d	1/3	2/3	1/2	139(2)	U_{11}	117(3)	69(1)	131(1)
Mg	3g	0.2375(3)	0	1/2	119(8)	109(9)	145(10)	54(5)	125(4)
CePtMg									
Ce	3f	0.414 44(9)	0	0	102(2)	107(3)	101(2)	53(1)	103(1)
Pt1	1a	0	0	0	117(2)	U_{11}	86(3)	58(1)	106(1)
Pt2	2d	1/3	2/3	1/2	107(1)	U_{11}	97(2)	53(1)	103(1)
Mg	3g	0.7612(5)	0	1/2	84(12)	95(17)	82(17)	48(8)	86(7)
CeAuMg									
Ce	3f	0.585 03(6)	0	0	116(2)	116(2)	130(2)	58(1)	120(1)
Au1	1a	0	0	0	134(1)	U_{11}	113(2)	67(1)	127(1)
Au2	2d	1/3	2/3	1/2	121(1)	U_{11}	124(2)	60(1)	122(1)
Mg	3g	0.2410(4)	0	1/2	101(9)	87(12)	134(12)	44(6)	109(5)

[a] $U_{\rm eq}$ is defined as one third of the trace of the orthogonalized U_{ij}-tensor. The anisotropic displacement factor exponent takes the form: $-2\pi[(ha^*)^2U_{11} + \cdots + 2hka^*b^*U_{12}]$. $U_{13} = U_{23} = 0$.

a refined occupancy parameter of 110% indicating a homogeneity range. This site was subsequently refined with mixed magnesium/palladium occupancy resulting in the composition $CePd_{1.03(1)}Mg_{0.97(1)}$ for the crystal investigated. Subsequently, we also investigated a crystal taken from the 1:1:1 sample. This CePdMg single crystal showed full occupancy of all sites within one standard deviation and there was no indication for a mixed occupancy. The results of this refinement are listed in tables 2–4. Final difference Fourier syntheses were flat and

Table 4. Interatomic distances (pm), calculated with the lattice parameters taken from x-ray powder data for CePdMg, CePtMg, and CeAuMg.

	CePdMg				CePtMg				CeAuMg		
Ce:	4	Pd2	308.7[a]	Ce:	4	Pt2	307.4	Ce:	4	Au2	314.2
	1	Pd1	319.5		1	Pt1	312.9		1	Au1	321.2
	2	Mg	335.6		2	Mg	333.7		2	Mg	339.7
	4	Mg	345.2		4	Mg	341.8		4	Mg	350.0
	4	Ce	399.4		4	Ce	393.7		4	Ce	403.5
	2	Ce	410.4		2	Ce	413.8		2	Ce	421.6
Pd1:	6	Mg	274.4	Pt1:	6	Mg	274.4	Au1:	6	Mg	281.5
	3	Ce	319.5		3	Ce	312.9		3	Ce	321.2
Pd2:	3	Mg	299.4	Pt2:	3	Mg	294.0	Au2:	3	Mg	300.2
	6	Ce	308.7		6	Ce	307.4		6	Ce	314.2
Mg:	2	Pd1	274.4	Mg:	2	Pt1	274.4	Mg:	2	Au1	281.5
	2	Pd2	299.4		2	Pt2	294.0		2	Au2	300.2
	2	Mg	315.6		2	Mg	312.3		2	Mg	323.1
	2	Ce	335.6		2	Ce	333.7		2	Ce	339.7
	4	Ce	345.2		4	Ce	341.8		4	Ce	350.0

[a] All distances within the first coordination spheres are listed. Standard deviations are equal to or less than 0.4 pm.

revealed no significant residual peaks. Atomic coordinates and interatomic distances are listed in tables 3 and 4. Listings of the structure factor tables are available[3].

3.2. Crystal chemistry and chemical bonding

The lanthanum and cerium compounds LaPdMg, CePdMg, LaPtMg, CePtMg, LaAuMg, and CeAuMg crystallize with the ZrNiAl structure [23, 24], a ternary ordered variant of the Fe_2P type [25, 26]. LaPtMg, CePtMg, LaAuMg, and CeAuMg are reported herein for the first time, while x-ray powder data have already been reported for LaPdMg and CePdMg by Iandelli [10].

As an example, the CeAuMg structure is presented in figure 1. The different tri-capped trigonal prismatic sites, i.e. $[Au1Mg_6Ce_3]$ and $[Au2Ce_6Mg_3]$, are emphasized. The cerium atoms have coordination number (CN) 17, with six cerium, five gold, and six magnesium atoms. The Ce–Ce distances in the CeTMg (T = Pd, Pt, Au) compounds range from 394 to 422 pm, much longer than in fcc cerium [27] where each cerium atom has 12 cerium neighbours at 365 pm. These Ce–Ce distances are well above the Hill limit [28] of about 340 pm for f-electron localization, in agreement with the magnetic ordering discussed below.

The shortest Pd–Mg, Pt–Mg, and Au–Mg distances in CePdMg, CePtMg, and CeAuMg are 274, 274, and 282 pm, slightly longer than the sums of Pauling's single-bond radii [29] of 265, 266, and 270 pm, respectively. These transition metal–magnesium contacts have most probably moderate bonding character.

Magnesium–magnesium bonding certainly plays an important role in the CeTMg compounds. The Mg–Mg distances within the triangular planes of the $[T1Mg_6Ce_3]$ prisms are 316, 312, and 323 pm in CePdMg, CePtMg, and CeAuMg, respectively. These bond lengths compare well with average Mg–Mg distances of 320 pm in hcp magnesium [27]. For a more detailed view of the crystal chemistry and chemical bonding in such Fe_2P-related intermetallic compounds we refer the reader to [15, 20, 22]. Finally, we briefly comment on the

[3] Details may be obtained from: Fachinformationszentrum Karlsruhe, D-76344 Eggenstein–Leopoldshafen (Germany), by quoting the Registry Nos CSD-412400 (CePdMg), CSD-412401 (CePtMg), and CSD-412402 (CeAuMg).

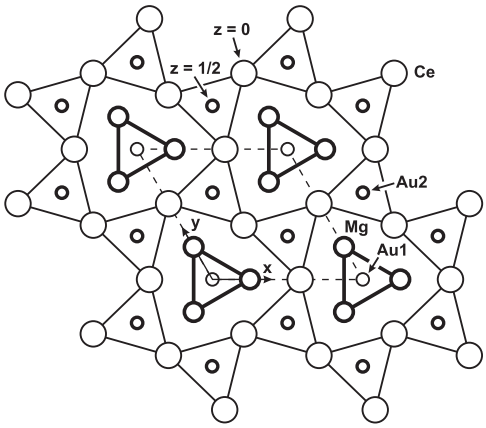

Figure 1. Crystal structure of CeAuMg projected onto the xy-plane. All atoms lie on mirror planes at $z = 0$ and $1/2$, indicated by the thin and thick lines, respectively. The trigonal prisms around the gold atoms are emphasized.

small homogeneity range of CePdMg. Refinement of the occupancy parameters of a crystal from the starting composition Ce:Pd:Mg = 2:2:1 showed a composition $CePd_{1.03(1)}Mg_{0.97(1)}$, indicating a small homogeneity range, $CePd_{1+x}Mg_{1-x}$, with a statistical palladium occupancy on the magnesium site. The lattice parameters of our CePdMg samples, however, were all identical within two standard deviations. Similar behaviour has recently also been observed for several gold- and silver-containing intermetallics with the same structure type [30, 31]. Since the palladium atoms are more electronegative than the magnesium atoms, such a partial Mg/Pd substitution also has an influence on the electronic behaviour of the cerium atoms and may therefore change the magnetic behaviour.

3.3. Magnetic susceptibility

The temperature dependences of $1/\chi_{mol}$ for CeTMg (T = Pd, Pt, Au) in external fields of $H_{ext} = 1$ T are presented in figure 2. Above ≈100 K the magnetic susceptibilities of all three compounds obey a Curie–Weiss law, $\chi_{mol} = C/(T - \Theta_P)$, where Θ_P is the paramagnetic Curie temperature and $C = \frac{N}{V}\frac{\mu_{eff}^2}{3\mu_0 k_B}$ is the Curie constant. The results of the fits to the data give $\Theta_P = -36(1)$, $-35(1)$, and $-57(1)$ K and $\mu_{eff}^{exp} = 2.6(1)$, 2.5(1), and 2.6(1) μ_B for CePdMg, CePtMg, and CeAuMg, respectively. The values of μ_{eff}^{exp} for all three compounds are in close agreement with the theoretical value of $\mu_{eff} = 2.54\ \mu_B$ expected for free Ce^{3+} ions (ground-state configuration $^2F_{5/2}$). Below ≈50 K large deviations from the Curie–Weiss law are observed, indicating the point at which crystal electric field effects become important.

The susceptibilities of CeTMg (T = Pd, Pt, Au) measured in an external field of $H_{ext} = 0.1$ T below 10 K are plotted in figure 3. CePdMg and CePtMg order magnetically with a sharp increase of the magnetic susceptibility with ordering temperatures $T_C = 2.1(2)$, and 3.6(2) K, respectively. These results contradict the previous work of Geibel *et al* [13], who did not observe any magnetic transition down to 2 K in CePdMg. A possible explanation for this different magnetic behaviour could be the homogeneity range in $CePd_{1+x}Mg_{1-x}$ as discussed above.

A sharp maximum in the susceptibility of CeAuMg at $T_N = 2.0(1)$ K indicates antiferromagnetic ordering. In order to determine the nature of the magnetic ordering in

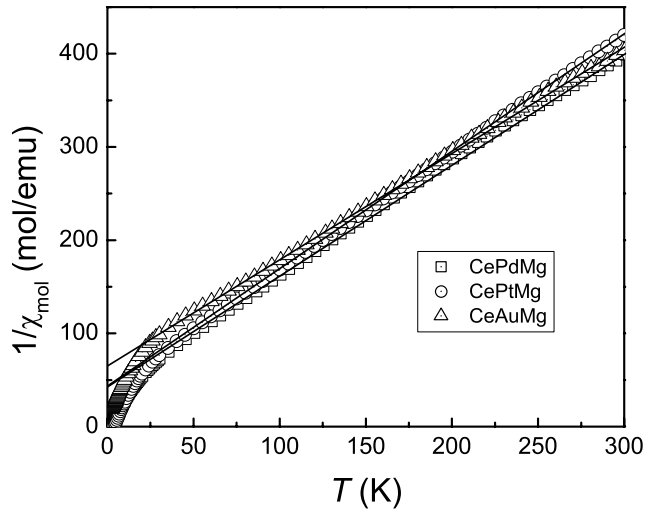

Figure 2. Temperature dependences of the inverse magnetic susceptibilities of CePdMg, CePtMg, and CeAuMg. The full lines represent fits to the Curie–Weiss law above 100 K and extrapolated to 0 K.

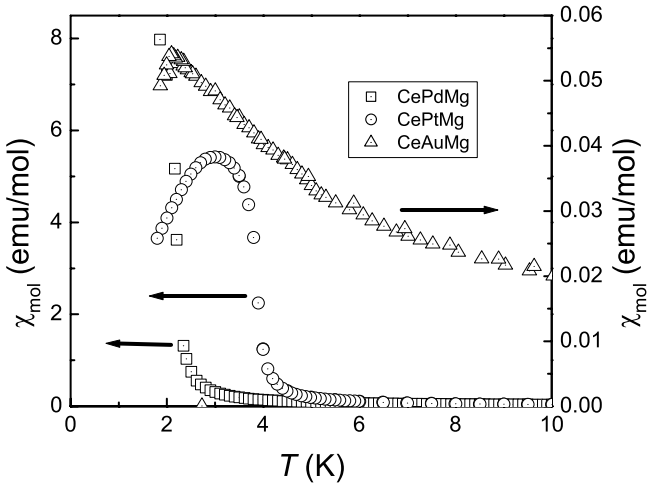

Figure 3. Temperature dependences of the dc magnetic susceptibilities of CePdMg, CePtMg, and CeAuMg below 10 K.

CePdMg and CePtMg we have measured magnetization isotherms for both compounds up to $H_{ext} = 7$ T and 300 K. As an example we show the magnetization curves of CePtMg in figure 4. Below T_C there is a typical sharp rise in magnetization with increasing field. However, full saturation of the magnetic moment is not observed up to 7 T. This could be an indication of a complex ordering pattern with spin canting involved. However, there are several other possibilities for the occurrence of such an effect that cannot be ruled out. These include averaging effects on the polycrystallites, the influence of the crystal field which could reduce the intrinsic moment associated with the doublet ground state, or even a small amount of hybridization (e.g. Kondo effect) which is not large enough to entirely remove the magnetic ordering.

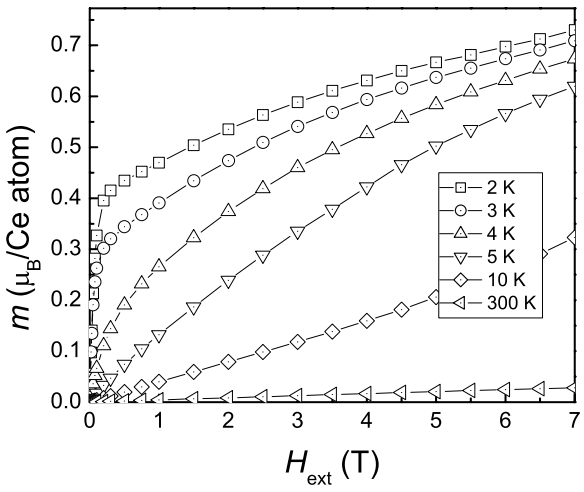

Figure 4. Selected magnetization isotherms between 2 and 300 K for CePtMg.

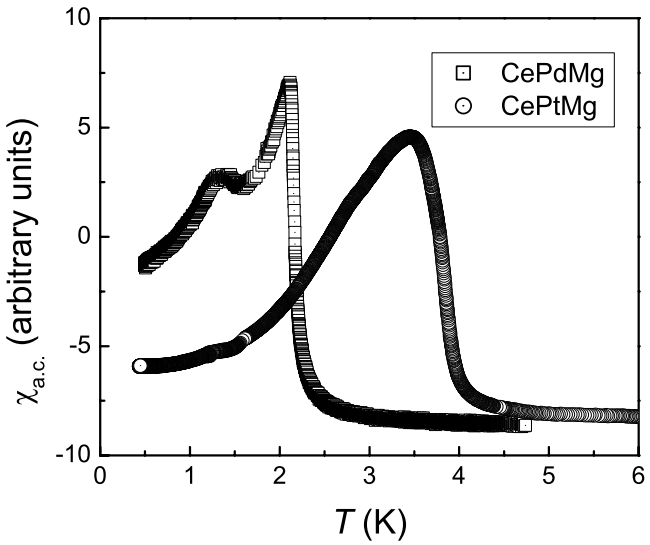

Figure 5. χ_{ac} for CePdMg and CePtMg below 6 K.

Further measurements have been made on CePtMg and CePdMg down to $T = 0.3$ K using a ^{3}He cryostat. The results of these χ_{ac}-measurements are presented in figure 5 and show magnetic transitions at $T_N = 2.2(2)$ and $T_N = 3.7(2)$ K, respectively in good agreement with the reported χ_{dc}-measurements. An examination of the second harmonic of χ_{ac} supports our assumption of magnetic transitions in both compounds containing large ferromagnetic contributions in both cases. Of particular interest is CePdMg which shows a second broad anomaly at $T \approx 1.2$ K. Such behaviour is quite common in RE intermetallics (see e.g. [32]) and at present we ascribe it to further magnetic reordering of the magnetic moments at this temperature.

All three LaTMg (T = Pd, Pt, Au) compounds show Pauli paramagnetic behaviour down to temperatures of $T = 0.3$ K with no indication of bulk superconducting behaviour, as seen

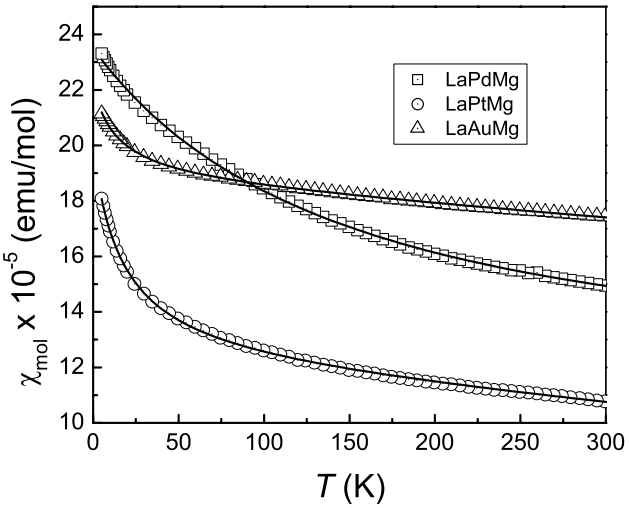

Figure 6. Temperature dependences of the dc magnetic susceptibilities of LaPdMg, LaPtMg, and LaAuMg in external fields of $H_{ext} = 7$ T.

from both χ_{dc}- and χ_{ac}-measurements. In figure 6 we show χ_{dc}-results measured in external fields of $H_{ext} = 7$ T. In all cases substantial Curie-type contributions are observed below $\approx$100 K which most probably arise from paramagnetic impurities. However, we can gain an approximate value for the Pauli paramagnetism by fitting the experimental data to the equation

$$\chi = \frac{C}{(T - \Theta_P)} + \chi_0 \tag{1}$$

where $C/(T - \Theta_P)$ ($\Theta_P \approx -10$ K in all cases) is a Curie term accounting for the magnetic impurities and $\chi_0 = \chi_P + \chi_{dia}$ is the sum of Pauli and diamagnetic susceptibility terms. Fits to the data give $\chi_0 \approx 100 \times 10^{-6}$, 120×10^{-6}, and 190×10^{-6} emu mol^{-1} for LaPdMg, LaPtMg, and LaAuMg, respectively. χ_{dia} can in theory be subtracted to extract χ_P assuming that χ_{dia} is the sum of individual diamagnetic increments. This approach only really works for simple ionic insulating compounds. However, we use this method here to derive approximate values for χ_P. Increments for the complex polyanions (TMg^{3-}) are not available [33] so we use the ionic increments [34] ($\times 10^{-6}$ emu mol^{-1}) for La: -30, Pd: -18, Pt: -28, Au: -32, Mg: -3. Subtracting the sum of the χ_{dia} gives $\chi_P = 151 \times 10^{-6}$, 181×10^{-6}, and 255×10^{-6} emu mol^{-1} for LaPdMg, LaPtMg, and LaAuMg, respectively. χ_P is then proportional to the density of states from $\chi_P = \mu_B^2 N(E_F)$. The calculated values of χ_P are listed in table 6. The results are too approximate (due to the large paramagnetic upturn and the imprecise values of χ_{dia}) to allow us to derive meaningful values of $N(E_F)$ from our susceptibility data. However, it is seen that there is at least good qualitative agreement with the relative magnitudes of χ_P and $N(E_F)$ as derived from heat capacity measurements in the next section.

3.4. Heat capacity

The heat capacity measurements of CePdMg, CePtMg, and CeAuMg are shown in figure 7. Phase transitions in the heat capacities are observed at $T = 2.0(1)$ K (CePdMg), $T = 3.6(1)$ K (CePtMg), and $T = 2.1(1)$ K (CeAuMg), corresponding closely to the magnetic transitions detected in the respective susceptibility measurements.

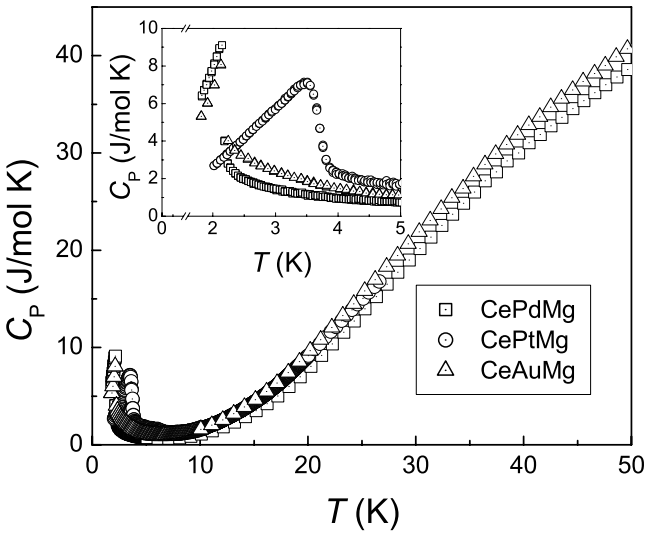

Figure 7. Heat capacities of magnetic CePdMg, CePtMg, and CeAuMg at low temperatures.

Table 5. Magnetic data for the $S = 1/2$ intermetallic compounds, CePdMg, CePtMg, and CeAuMg as derived from susceptibility and heat capacity measurements.

Compound	$T_{C/N}$ (K)	μ_{eff}^{exp} (μ_B)	Θ_P (K)	Reference
CePdMg	< 2 K	2.6	−33	[13]
CePdMg	2.1(2)	2.6(1)	−36(1)	This work
CePtMg	3.6(2)	2.5(1)	−35(1)	This work
CeAuMg	2.0(2)	2.6(1)	−57(1)	This work

Table 6. Data for non-magnetic LaTMg (T = Pd, Pt, Au) as derived from heat capacity and susceptibility measurements.

Compound	γ (mJ mol^{-1} K^{-2})	N_F (eV^{-1}) (from C_P)	χ_0 (10^{-6}	χ_P emu mol^{-1})	$\Theta_D(0)$ (K)
LaPdMg	7.48	3.18	100	151	218
LaPtMg	8.65	3.67	120	181	203
LaAuMg	9.03	3.83	190	255	176

The total heat capacity of each compound can be considered to be composed of three contributions;

$$C_P(T) = C_{latt}(T) + C_{el}(T) + C_{4f}(T) \tag{2}$$

where $C_{latt}(T)$ is the lattice contribution and $C_{el}(T) = \gamma T$ is the contribution from conduction electrons. The term C_{4f} arises from magnetic contributions of the localized Ce^{3+} 4f moments (see figure 9 for example).

In order to separate the individual terms, the lattice and electronic contributions have been derived from the heat capacities of isostructural and non-magnetic LaTMg (T = Pd, Pt, Au), respectively. Because the molar masses and lattice parameters of the magnetic and non-magnetic compounds are very similar, we did not apply any scaling corrections for the slightly different molar masses of the compounds.

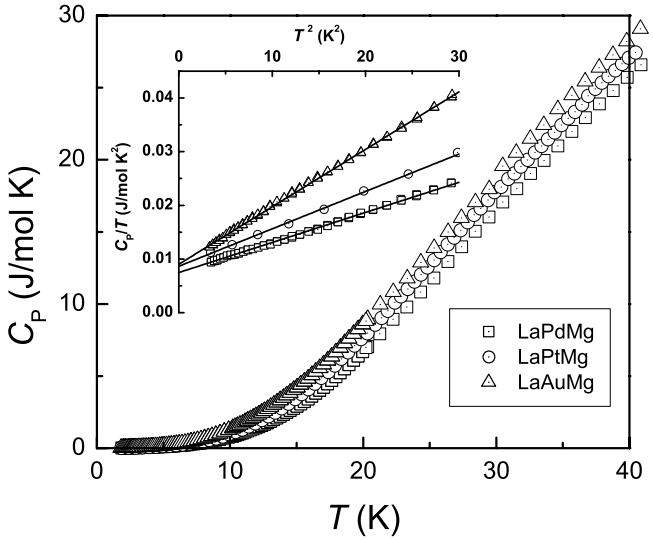

Figure 8. Heat capacities of non-magnetic LaPdMg, LaPtMg, and LaAuMg. The inset shows the least-squares fits to the heat capacity below ≈6 K.

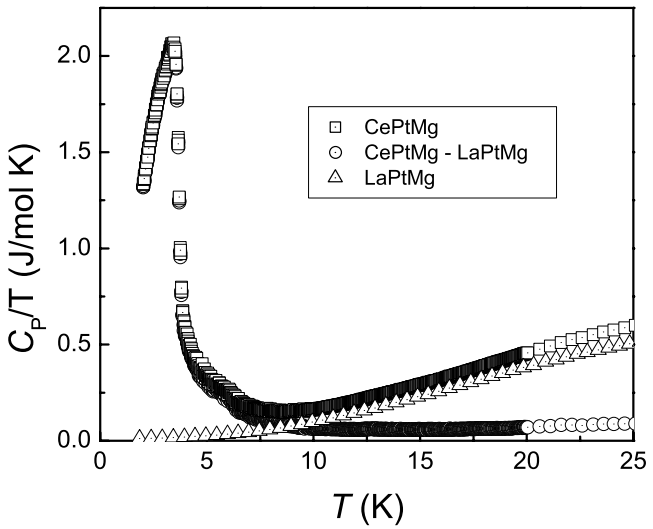

Figure 9. Heat capacity of CePtMg: separated of C_P into individual components. LaPtMg was used to approximate the non-magnetic contributions.

The heat capacities of LaPdMg, LaPtMg, and LaAuMg are shown in figure 8. At low temperatures ($T < 5$ K) the lattice and electronic contributions may be approximated as the sum of the Debye T^3-term and a linear Sommerfeld term;

$$C_P = \gamma T + \beta T^3 \tag{3}$$

where $\gamma = \frac{1}{3}\pi N(E_F)k_B^2$ and $\beta \approx 12\pi^4/5Rn(\frac{1}{\Theta_D(0)})^3$ with the individual terms having their usual meanings.

The electronic terms and initial Debye temperatures ($\Theta(0)$) are obtained from low-temperature fits of C_P/T versus T^2 as shown in figure 8, inset. These are listed in table 6

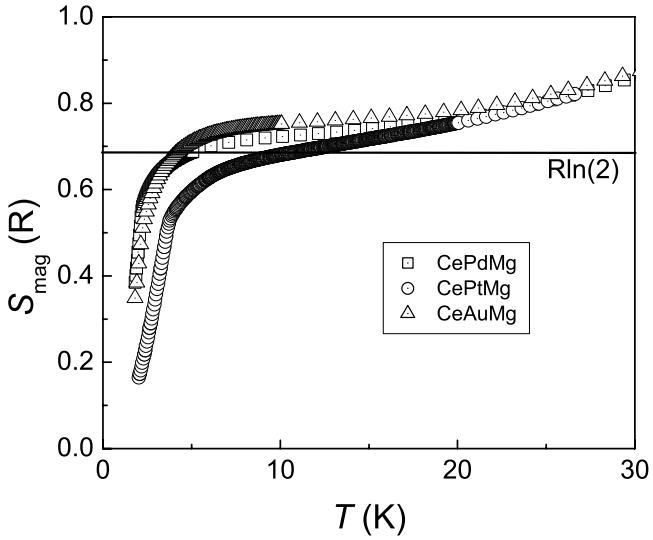

Figure 10. Magnetic entropies of CePdMg, CePtMg, and CeAuMg in units of R. The solid horizontal line depicts $R\ln(2)$, the value of a doublet ground state.

for the respective compounds. It is seen that the γ-values are similar for all compounds, $\approx$8 mJ mol^{-1} K^{-2}. The Debye temperatures however depend strongly upon the low-frequency vibrations of the transition metal atoms. The largest $\Theta_D(0)$ occurs for LaPdMg which has the lowest mass, and the smallest for LaAuMg, which has the greatest mass.

From our analysis of CeTMg (T = Pd, Pt, Au) it is impossible to extract a value of γ due to the low magnetic ordering temperature of these compounds. We therefore assume that the γ-values are very similar to those for the isotypic LaTMg compounds.

The contribution $C_{4f}(T)$, after subtraction of C_{el} and C_{latt}, for CePtMg is shown as an example in figure 9. $C_{4f}(T)$ contains the peaks resulting from the magnetic ordering of the Ce ions, and a superimposed Schottky anomaly above T_C which has a broad maximum at $T_{Sch} \approx 30$ K (not shown in figure 9). Ce^{3+} is a $^2F_{5/2}$ Kramers ion, and is therefore expected to split into $(2J + 1)/2 = 3$ Kramers doublets.

The magnetic entropies of CePdMg, CePtMg, and CeAuMg are plotted in figure 10, as calculated from the integral over the magnetic contribution to the specific heat capacity:

$$S_{mag} = \int_0^\infty \frac{C_{mag}}{T}\,dT \tag{4}$$

where S_{mag}, the magnetic entropy, is plotted in figure 10 in units of R, the gas constant. In order to estimate the remaining magnetic entropy contribution between 0 and 1.5 K we fitted curves of T^2 to the low-temperature side of the C_P-jump, and extrapolated down to 0 K. For all three compounds, S_{mag} increases steeply and levels out at $T \approx 10$ K, corresponding to a value close to $R\ln(2)$, and increasing again at higher temperatures. This indicates that all three compounds have a doublet ground state, with the first excited states lying above the ground states ($\approx$75 K) as indicated by the maximum temperature of the crystal field Schottky anomaly.

3.5. Electrical resistivity

The temperature dependences of the normalized ($\rho(T)/\rho(300\ \mathrm{K})$) electrical resistivities for CePdMg, CePtMg, and CeAuMg are presented in figure 11. The resistivities are observed to

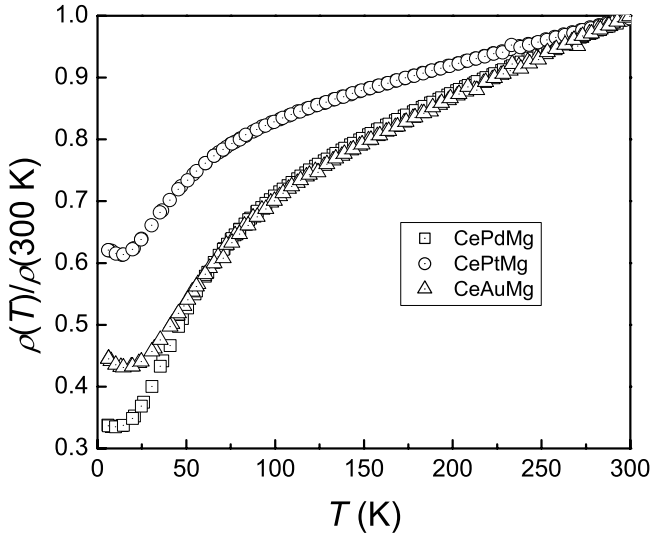

Figure 11. Electrical resistivities of CePdMg, CePtMg, and CeAuMg as a function of temperature.

decrease with decreasing temperature in correspondence with metallic behaviour. Negative curvature of $\rho(T)$ is observed for all three compounds below ≈100 K, which could arise from CEF level population which causes an additional temperature dependence of the spin disorder resistivity [35]. However, we observe similar, but less pronounced, negative curvature of $\rho(T)$ within non-magnetic LaTMg (not shown).

4. Conclusions

We have presented in this paper a detailed investigation of the crystal structure and physical properties of the ternary intermetallic compounds, RETMg (RE = La, Ce; T = Pd, Pt, Au). Previously, only the x-ray powder diffraction of LaPdMg and CePdMg [10], and the magnetic susceptibility of CePdMg [13] have been studied.

Single-crystal x-ray diffraction shows that all of our compounds in the series RETMg crystallize with the ZrNiAl structure, which is a ternary ordered variant of the well known Fe_2P type. We have examined the physical properties of these compounds in some depth in order to check for the possible occurrence of instabilities in the Ce 4f configuration. Our susceptibility and heat capacity measurements show that the compounds CePdMg, CePtMg, and CeAuMg all exhibit long-range magnetic order at low temperatures. CePdMg and CePtMg order magnetically at $T_C = 2.1(2)$ and 3.6(2) K, respectively. CePdMg also displays an intriguing second transition at $T \approx 1.2$ K, most probably resulting from a reordering of the Ce magnetic moments. CeAuMg orders antiferromagnetically at $T_N = 2.0(2)$ K. From the fits to the high-temperature susceptibilities we find for CePdMg, CePtMg, and CeAuMg that the Ce ions are in the Ce^{3+} ground state. The lanthanum compounds are all Pauli paramagnets.

Heat capacity measurements confirm the observation of long-range magnetic ordering in CeTMg (T = Pd, Pt, Au) in good agreement with our susceptibility results. An examination of the magnetic entropies suggests doublet ground states, as expected for Ce^{3+} ions, with the next excited states at ≈75 K.

Acknowledgments

We thank Dipl-Ing U Ch Rodewald for the diffractometer measurements, E Brücher for the susceptibility measurements, G Siegle for the resistivity and heat capacity measurements, and A Fugmann for experimental help. Special thanks go to Degussa-Hüls AG for generous gifts of the noble metals. This work was in part financially supported by the Deutsche Forschungsgemeinschaft, by the Fonds der Chemischen Industrie, and by the Bennigsen-Foerder-Programm of the Ministerium für Wissenschaft und Forschung des Landes Nordrhein-Westfalen.

References

[1] Rogl P, Chevalier B, Besnus M J and Etourneau J 1989 *J. Magn. Magn. Mater.* **80** 305
[2] Fujita T, Suzuki T, Nishigori S, Takabatake T, Fujii H and Sakurai J 1992 *J. Magn. Magn. Mater.* **108** 35
[3] Szytula A and Leciejewicz J 1994 *Handbook of Crystal Structures and Magnetic Properties of Rare-Earth Intermetallics* (Boca Raton, FL: Chemical Rubber Company)
[4] Kaczorowski D, Rogl P and Hiebl K 1996 *Phys. Rev.* B **54** 9891
[5] Gordon R A and DiSalvo F J 1996 *J. Alloys Compounds* **238** 57
[6] Laffargue D, Fourgeot F, Bourrée F, Chevalier B, Roisnel T and Etourneau J 1996 *Solid State Commun.* **100** 575
[7] Niepmann D, Pöttgen R, Künnen B and Kotzyba G 2000 *J. Solid State Chem.* **150** 139
[8] Pöttgen R, Fugmann A, Hoffmann R-D, Rodewald U Ch and Niepmann D 2000 *Z. Naturf.* b **55** 155
[9] Berger G and Weiss A 1988 *J. Less-Common Met.* **142** 109
[10] Iandelli A 1994 *J. Alloys Compounds* **203** 137
[11] Horechyy A I, Pavlyuk V V and Bodak O I 1999 *Pol. J. Chem.* **73** 1681
[12] Johrendt D, Trill H and Fickenscher F 2002 *J. Solid State Chem.* **164** 201
[13] Geibel C, Klinger U, Weiden M, Buschinger B and Steglich F 1997 *Physica* B **237** 202
[14] Pöttgen R, Gulden Th and Simon A 1999 *GIT Labor-Fachz.* **43** 133
[15] Pöttgen R, Lang A, Hoffmann R-D, Künnen B, Kotzyba G, Müllmann R, Mosel B D and Rosenhahn C 1999 *Z. Kristallogr.* **214** 143
[16] Yvon K, Jeitschko W and Parthé E 1977 *J. Appl. Crystallogr.* **10** 73
[17] Hwang J S, Lin K and Tien C 1997 *Rev. Sci. Instrum.* **68** 94
[18] van der Pauw L J 1958 *Philips Res. Rep.* **13** 1
[19] Pöttgen R, Kotzyba G, Görlich E A, Łatka K and Dronskowski R 1998 *J. Solid State Chem.* **141** 352
[20] Sheldrick G M 1997 *SHELXL-97, Program for Crystal Structure Refinement* University of Göttingen
[21] Flack H D and Bernadinelli G 1999 *Acta Crystallogr.* A **55** 908
[22] Bernadinelli G and Flack H D 2000 *J. Appl. Crystallogr.* **33** 1143
[23] Krypyakevich P I, Markiv V Ya and Melnyk E V 1967 *Dopov. Akad. Nauk Ukr. RSR* A 750
[24] Zumdick M F, Hoffmann R-D and Pöttgen R 1999 *Z. Naturf.* b **54** 45
[25] Rundqvist S and Jellinek F 1959 *Acta Chem. Scand.* **13** 425
[26] Zumdick M F and Pöttgen R 1999 *Z. Kristallogr.* **214** 90
[27] Donohue J 1974 *The Structures of the Elements* (New York: Wiley)
[28] Hill H H 1970 *Plutonium and Other Actinides (Nuclear Materials Series vol 17)* ed W N Mines (New York: AIME) p 2
[29] Pauling L 1960 *The Nature of the Chemical Bond and the Structures of Molecules and Crystals* (Ithaca, NY: Cornell University Press)
[30] Pöttgen R, Hoffmann R-D, Renger J, Rodewald U Ch and Möller M H 2000 *Z. Anorg. Allg. Chem.* **626** 2257
[31] Fickenscher Th and Pöttgen R 2001 *J. Solid State Chem.* **161** 67
[32] Gibson B J, Pöttgen R, Schnelle W, Ouladdiaf B and Kremer R K 2001 *J. Phys.: Condens. Matter* **13** 2593
[33] Schnelle W, Pöttgen R, Kremer R K, Gmelin E and Jepsen O 1997 *J. Phys.: Condens. Matter* **9** 1435
[34] Selwood P W 1956 *Magnetochemistry* (New York: Interscience)
[35] Gratz E and Zuckermann M J 1983 Transport properties of rare-earth intermetallic compounds *Handbook on the Physics and Chemistry of Rare-Earths* vol 5, ed K A Gschneidner Jr and L Eyring (Amsterdam: North-Holland) p 117